

# Ruthenium Polypyridine Complexes. On the Route to Biomimetic Assemblies as Models for the Photosynthetic Reaction Center

HEINZ DÜRR\*<sup>†</sup> AND STEFAN BOSSMANN<sup>‡</sup>

Fak. 8.12, Organische Chemie, Universität des Saarlandes, 66041 Saarbrücken, Germany, and Engler-Bunte-Institut, Universität Karlsruhe, Engler-Bunte-Ring, 1,76128 Karlsruhe, Germany

Received September 21, 2000

## ABSTRACT

We describe in this Account the preparation of RuL<sub>3</sub> complexes and their significance as biomimetic models for the photosynthetic reaction center. Their preparation from simple or more complicated polypyridine ligands L and their photophysical data, especially their stability, are reported. Biomimetic models involving three concepts of the interaction of RuL<sub>3</sub> with acceptors in coordinatively, mechanically, or covalently linked supramolecular assemblies are also presented. The electron transfer (ET) of the noncovalently linked assemblies of RuL<sub>3</sub> complexes carrying polyether chains with one or two anisyl binding sites (**4** or **5**) with the cyclic bisviologen was studied. Molecular modeling and NMR titration clearly show the formation of supramolecular assemblies. Time-resolved spectroscopy demonstrated that ET and charge separation in the RuL<sub>3</sub> complexes with two binding sites are more efficient. The more constrained RuL<sub>3</sub>–bisviologen–catenane (**6**) possesses two conformations which exhibit different efficiency in ET, creating a charge-separated state in the microsecond domain. The covalently linked Ru(bpy)<sub>3</sub><sup>2+</sup>–viologen assemblies having one (**7**, diad) or two bisviologen arms (**8**, diad) result in efficient ET. Addition of linear polyethers, cyclic polyethers, or crowns generates new triads and tetrads of the pseudorotaxane type. Molecular modeling and NMR titration clearly indicate the formation of supramolecular assemblies. The analysis of time-resolved studies proves fast ET and especially long-lived charge-separated states in these pseudorotaxanes. These data, compared with the findings for the photosynthetic reaction center, show conclusive results. The lifetimes of the charge-separated states increase clearly in the sequence for noncovalently < mechanically < and covalently linked assemblies.

## Introduction

Photosynthesis converts only 0.02–0.05% of the incident solar energy of about 10<sup>22</sup> kJ/year into biological material.

Heinz Dürr is Professor at the Naturwissenschaftlich Technische Fakultät III, 8.12 Organische Chemie, at the Universität des Saarlandes, Saarbrücken, Germany. Dr. Dürr received his Vordiplom from the Technical University of Stuttgart in 1956, his Diplom in chemistry at the University of Heidelberg in 1959, and his Ph.D. in organic chemistry at Heidelberg in 1961. Dr. Dürr carried out postdoctoral research at the Universities of Wisconsin–Madison and Strasbourg, France, and an industrial stay at the BASF Ludwigshafen until 1964. In 1969, Dr. Dürr received the Dr.Habil. in organic chemistry at the University of Saarland, Saarbrücken, and was promoted to Privatdozent in 1971. In 1971, he was promoted to Professor of organic chemistry at the University of Saarland, Saarbrücken. Dr. Dürr has served in the European Photochemistry Association as coeditor and on several boards. For many years he was the coordinator of the international student exchange programs in chemistry with France, England, and Greece. Since 1985, he has taught yearly at the ECPM-Strasbourg. In 1996, he received the Gay Lussac-Alexander Humboldt Award for French–German cooperation in science. His research interest includes carbene chemistry, photochemistry with special emphasis of photochromism and photoinduced (biomimetic) electron-transfer processes. Dr. Dürr has published 270 papers in scientific journals or books, 9 patents, and 3 books.

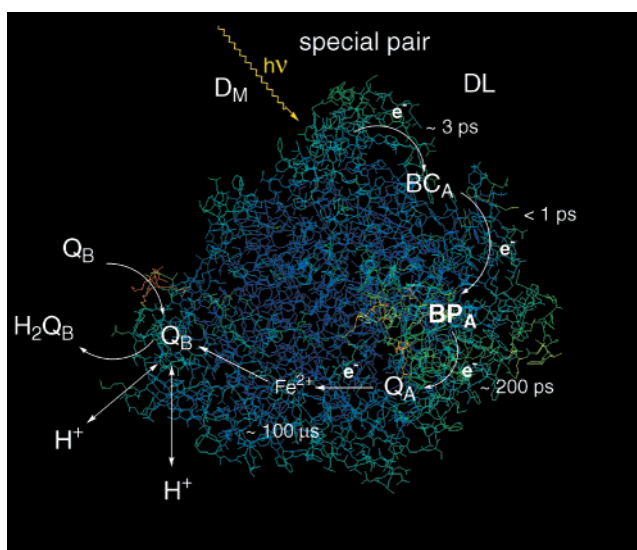


**FIGURE 1.** Reaction center (blue) of *Rhodobacter sphaeroides* including protein matrix (a) and simplified reaction center compounds (b) ( $D_M$ ,  $D_L$ ,  $B_{CA}$ ,  $B_{CB}$  = bacterio chlorophylls,  $B_{PA}$  and  $B_{PB}$  = pheophytins (not shown in Figure 1),  $Q_A$  and  $Q_B$  = quinones).

This is about 100 times more than the food needed for mankind.<sup>1</sup> Whereas in green or purple bacteria only one photosynthetic unit (PS II) is carrying out the light-to-chemical products conversion, green plants are using two systems (PS I and PS II). The essential process is water cleavage to O<sub>2</sub> and reduction of NADP to NADPH, which is used to finally produce sugars from CO<sub>2</sub> and H<sub>2</sub>O. The basis for the photosynthetic unit consists of the light-harvesting (LH) and the real photosynthetic unit (RC), which is depicted in Figure 1 schematically.

In the RC the light induced electron transfer, the decisive process for the formation of a long-lived primary charge-separated state of  $\tau = 100$  ns ( $D_C^+ \cdot B_{CA} Q_A Q_B^-$ ; see refs 1–3), initiating the consecutive chemical conversions.

The components of the photosynthetic RC and LH I and LH II absorb in purple bacteria between 500 nm (carotenoids) and 800–875 nm (bacteriochlorophylls). The energy transfer from LH II to the RC occurs in about 100 ps, with an efficiency of almost 1.

The photosynthetic reaction center was first characterized by Huber, Michel, and Deisenhofer in 1984 with the purple bacteria *Rhodospseudomonas viridis*.<sup>3</sup> The related *Rhodobacter sphaeroides* is almost identical<sup>3</sup> and is shown in Figure 1. Four bacteriochlorophylls D and BC as well as two pheophytines BP and quinones Q and Fe<sup>2+</sup> ion are fixed on the protein matrix noncovalently. The electron transfer occurs almost only via the L-branch<sup>3,4</sup> from  $D_C$

<sup>†</sup> Universität des Saarlandes.

<sup>‡</sup> Universität Karlsruhe.

Stefan Bossmann earned a doctoral degree (summa cum laude) in 1991 from the University of Saarland, Saarbrücken, Germany. From 1991 to 1993, he did postdoctorate work at Columbia University in New York City. From 1993 to 1999, he was “Hochschulassistent” (C1) at the University of Karlsruhe, Germany, where he earned the academic title “Privatdozent” in 1998. Since 1999, he has been “Hochschuldozent” (C2) at the University of Karlsruhe.

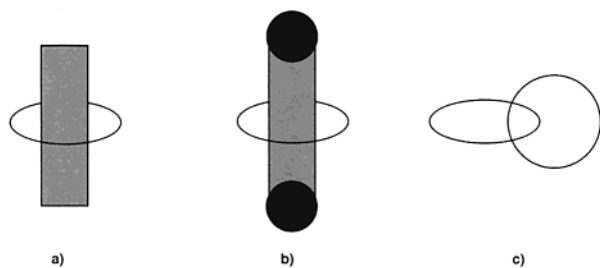


FIGURE 2. (a) [2]Pseudorotaxane, (b) [2]rotaxane, and (c) [2]-catenane.

$\rightarrow Q_A$  in less than 1 ns ( $Q_A \rightarrow Q_B \approx 100$  ms) with an efficiency of  $\sim 1$ .<sup>3,4</sup> The decisive charge-separated state has a lifetime of about 100 ms.

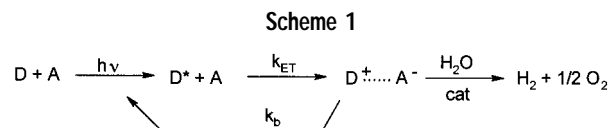
Self-organization of the components of the RC is one of the key features for its efficiency.

Supramolecular chemistry has shown in the past decade that noncovalent interactions such as solvophobic forces, electrostatic interactions with permanent or induced dipoles, dispersive and charge-transfer interactions, and hydrogen bonds can be used to induce self-organization in molecular components. Typical structures are shown in Figure 2.

A series of such systems based on noncovalent interactions being able to undergo light-induced electron transfer were described.<sup>4</sup>

The synthetically, often more complex, covalently linked systems will be dealt with in the second section (see also ref 4) of this paper. For these systems and their light-induced process, the term "artificial photosynthesis" was coined.

Natural as well as artificial photosynthesis possesses,<sup>5-7</sup> as primordial characteristics, efficient light-harvesting units for the conversion of solar energy. The basic reaction to be realized is light-induced charge separation leading to the cleavage of water. In artificial photosynthesis this is achieved by sensitizers *S* or donor *D* (*S* and *D* are used equivalently) absorbing in the visible region of the solar spectrum and by electron relays or acceptors *A* functioning as short-time reservoirs of chemical energy and redox-active components that can be used for energy storage.<sup>4</sup> The energy to be stored in a photoelectron-transfer reaction is based on the following processes. After excitation a ( $D^*A$ ) pair is generated. Electron transfer then produces ( $D^+A^-$ ). This pair can undergo a reaction to afford  $H_2$  and  $O_2$  from water or a competition reaction  $D^+ + A^-$  to  $DA$  occurs, the so-called back reaction. This leads to annihilation of the stored energy or, in other words, waste of energy. To avoid this problem a fast electron transfer is necessary. Looking for optimal systems thus means that both unimolecular and bimolecular light-induced processes should have high efficiency. The main task of modern research in the field of *artificial photosynthesis* is to better understand nature's processes by employing model compounds. A long-term goal is to generate biomimetic systems that carry out the photosynthetic reaction center's function to achieve water cleavage, as sketched in Scheme 1.



The basic component for such systems is a good sensitizer ( $S = D$ ) for electron transfer, such as porphyrins, ruthenium polypyridines, dyes, and semiconductors. In this Account we will treat first and exclusively functionalized ruthenium polypyridines and then more complex  $RuL_3$  (*D*)–viologen (*A*) polyads,<sup>6</sup> especially the ones developed in our group. With suitable acceptors such as viologens, electron transfer occurs in these systems.

All syntheses and photophysical studies including single photon counting were done in our group in Saarbrücken. The time-resolved spectra such as laser-induced nanosecond, picosecond, and femtosecond spectroscopy were carried out in collaboration with I. Willner, Jerusalem; A. Braun, Karlsruhe; N. J. Turro, New York; and F. De Schryver, Leuven.

The different ligands employed are based in principle on 2,2'-bipyridine derivatives or their bis-aza homologues. The 2,2'-bipyridines can be obtained from simple pyridine precursors<sup>5,6</sup> by direct coupling with Pd/C or LDA or Raney nickel from simple pyridines. A second route uses halopyridines and Cu(0) or Ni(0), and the third access employs Pd(0), halopyridines, and pyridyl-boric acids (Suzuki reaction). A complete construction of the second ring of 2,2'-bipyridines is possible with the Kröhnke reaction.<sup>5,6</sup>

Most efficiently, we employed the Pd route based on work of Tiecco et al.<sup>8</sup>

The substituents in the pyridines or bipyridines were introduced by modifying mostly  $CH_3$  groups to afford a large number of functional groups such as  $CH_2OH$ ,  $CH_2Br$ ,  $CHO$ ,  $COOH$ , and  $COOR$ . Thus, almost all necessary functionalities for further modification were accessible. More complex *D*–*A*-linked ligands<sup>6</sup> will be treated below. From these ligands  $RuL_3$  or  $RuL_2L$  complexes were prepared.<sup>6</sup>

Their photophysical data—especially with regard to electron transfer as donor *D*—and the extension of simple  $RuL_3$  complexes to supramolecular polyads acting as good sensitizers (*D*) depend on the following properties: absorption in the solar emission maximum, excited states with long lifetimes, suitable redox potentials, stability, fast inter- or intramolecular electron transfer.

The synthetic strategy we employed for ruthenium polypyridines<sup>6</sup> is shown in Scheme 2,<sup>6,8-17</sup> which shows a general method for the synthesis of trishomoleptic (such as *A*) and bisheteroleptic  $Ru(II)$  complexes (such as *B*) ( $DMSO =$  dimethyl sulfoxide,  $\lambda-\lambda =$  bpz = 1,4-bipyridazine, or  $\mu-\mu =$  bpy = 2,2'-bipyridine).

The  $RuL_3$  complexes show typical absorption in the region of 450 nm (MLCT = metal-to-ligand charge transfer) and 323 nm (MC = metal centered). The emission for the <sup>3</sup>(MLCT) state occurs normally at 630 nm with a lifetime of  $\tau = 600$  ns. The reduction potential of  $Ru(bpy)_3^{2+}$  is  $Ru^{*2+/3+}$ :  $-0.8$  V (in  $CH_3CN$  vs SCE). A

Scheme 2

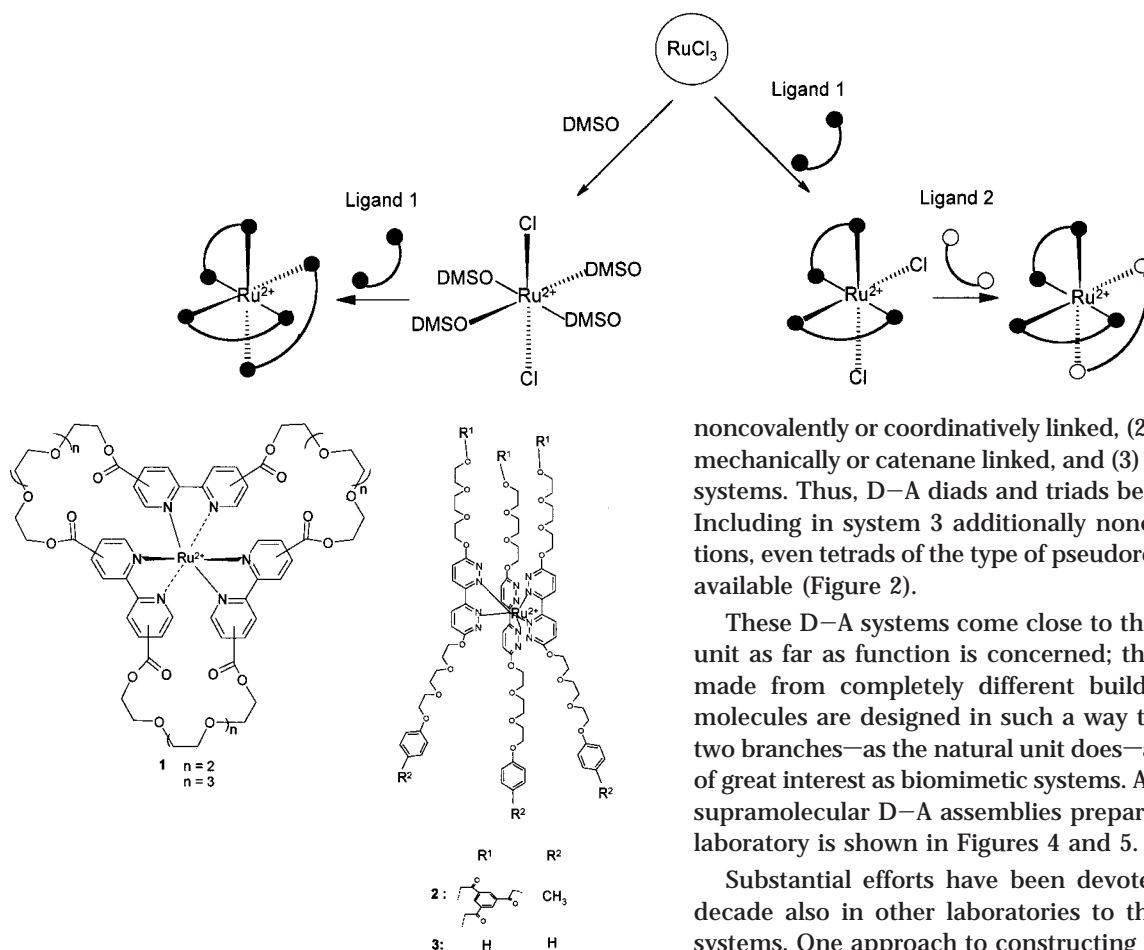


FIGURE 3. Typical fatigue-resistant Ru complexes 1–3.

multitude of  $\text{RuL}_3$  complexes have been made which vary little with these data.<sup>3–6</sup> The  $\text{RuL}_3$  complexes possess normally an octahedral structure as typical low-spin complexes.

### Ruthenium Polypyridines with Longer Lived Excited States

Longer lived excited states can—as we have shown—be synthesized by employing the less readily available bipyridazines.<sup>18</sup> The complexes made with this ligand show a large increase of  $\tau = 1\text{--}3 \mu\text{s}$ , making these complexes more efficient in electron-transfer processes. A few typical examples are collected in Figure 3 (for detailed photo-physical studies, see refs 10, 11, 13, 14, 16–18).

### Supramolecular Noncovalently or Mechanically and Covalently Linked Assemblies for Electron Transfer

Electron transfer in simple ruthenium polypyridine complexes to suitable acceptors A has been studied in detail.<sup>3–6</sup> We were interested in how far this process can be modified by the formation of different types of supramolecular assemblies. In these, three principal interactions of D–A assemblies are possible: (1) supramolecular

noncovalently or coordinatively linked, (2) supramolecular mechanically or catenane linked, and (3) covalently linked systems. Thus, D–A diads and triads become accessible. Including in system 3 additionally noncovalent interactions, even tetrads of the type of pseudorotaxanes become available (Figure 2).

These D–A systems come close to the photosynthetic unit as far as function is concerned; they are, however, made from completely different building blocks. Our molecules are designed in such a way that they contain two branches—as the natural unit does—and are therefore of great interest as biomimetic systems. A survey of typical supramolecular D–A assemblies prepared mostly in our laboratory is shown in Figures 4 and 5.

Substantial efforts have been devoted over the past decade also in other laboratories to the study of such systems. One approach to constructing artificial systems includes the syntheses of covalently linked donor–acceptor diads, triads,<sup>6</sup> tetrads,<sup>7</sup> and pentads.<sup>7</sup> In the following sections noncovalently, mechanically, and covalently as well as mixed linked systems are described.

### Noncovalently or Coordinatively Linked D–A Systems

Molecular modeling studies were carried out for two-shell complexes **4** and four-site complexes **5** as well as their host–guest complexes **4**/BXV<sup>4+</sup> (cyclic bisviologen, see Figure 4) and **5**/BXV<sup>4+</sup> (Figure 5).

The calculations show that the complexes formed are preferentially 1:1 complexes. The cyclophane BXV<sup>4+</sup> slides over the anisyl functions and resides in **4** on the only terminal anisyl. In **5**, however, two binding sites are possible, and the calculations show a folded geometry having BXV<sup>4+</sup> on the anisyl group (see Figure 4), creating thus a catenane-like pseudorotaxane structure (see Figure 5). These results are also confirmed by NMR titration studies.

### Electron-Transfer Studies of D–A Coronate Complexes

A first approach used in our group involved introducing crown ether cavities in suitable positions to bind the ruthenium polypyridine complexes.<sup>6b,c,11,14,19</sup> The structure

## COORDINATIVELY, MECHANICALLY AND COVALENTLY LINKED SUPRAMOLECULAR ASSEMBLIES

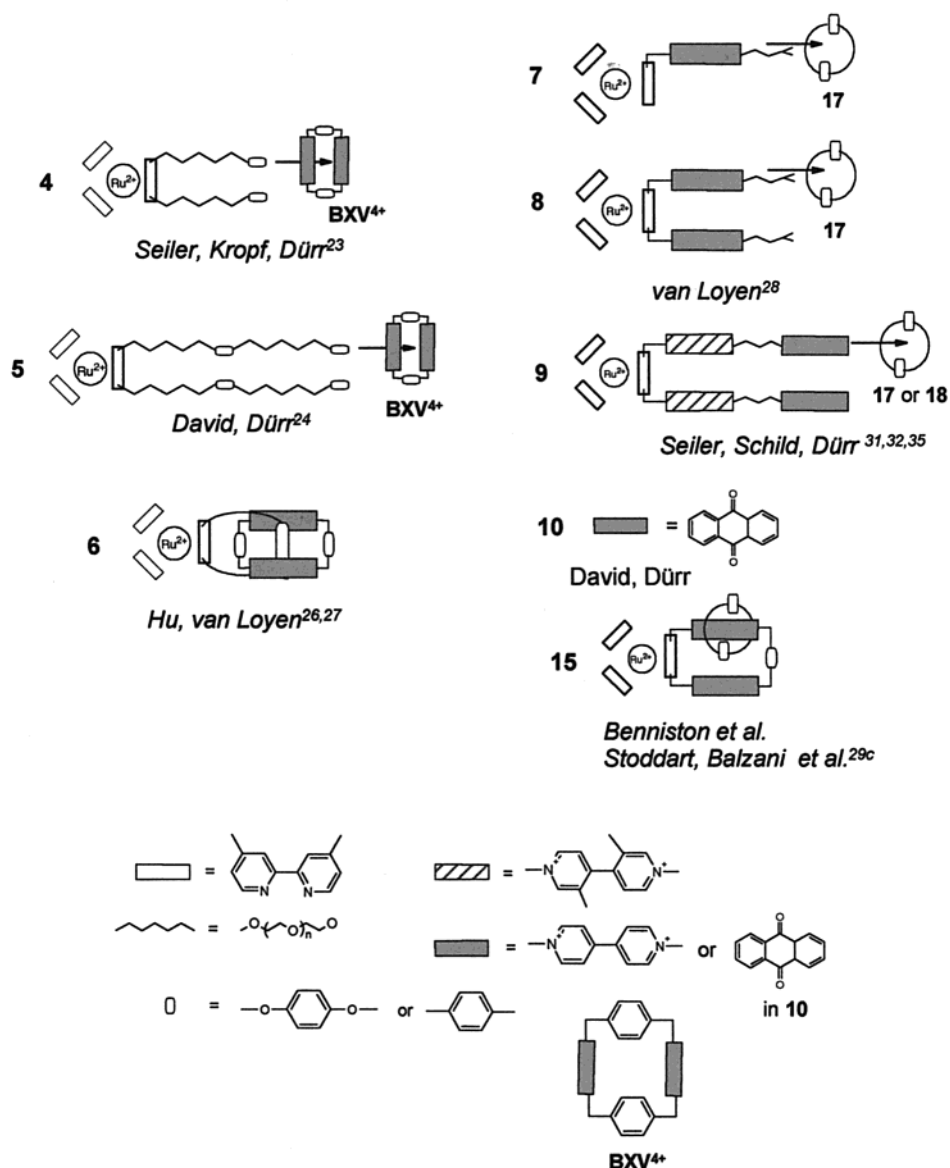


FIGURE 4. Coordinatively, mechanically, and covalently linked supramolecular assemblies.

of these complexes of the type **1** allows the interaction with quenchers such as MV<sup>2+</sup> (**13**, methylviologen) and OV<sup>2+</sup> (**14**, octylviologen). These molecules were studied by Stern–Volmer techniques.<sup>6d,19</sup> Nonlinear Stern–Volmer plots using the equation

$$\frac{I_0}{I} = 1 + k_q \tau_0 [Q]; \quad k_q = \text{quenching constant} \quad (1)$$

$$\frac{\tau_0}{\tau} = 1 + k_q \tau [Q] \quad (2)$$

$$\frac{I_0 \tau}{I \tau_0} = 1 + Kc [Q] \quad (3)$$

(definition of parameters: see Table 1)

for quenching are obtained, from which a supramolecular interaction was concluded.<sup>6b</sup>

The electron transfer in these systems can principally occur in the way shown in Scheme 3.

Electron-transfer studies with time-resolved techniques such as laser flash spectroscopy and single photon counting were carried out to experimentally substantiate this scheme.

The electron-transfer processes of **4** and **5** (Figure 3) (natural models) and **11** and **12** (Figure 5) with the quencher BXV<sup>4+</sup> (Stoddart relay, see Scheme 3) were studied by steady-state and time-resolved emission and absorption spectroscopy.<sup>23a,24,25</sup> The supramolecular assemblies **4**, **5**, **11**, and **12**/BXV<sup>4+</sup> can be classified as pseudorotaxanes. The data are shown in Table 1.

The steady-state luminescence quenching showed a clear nonlinearity in the Stern–Volmer plots of **5** and **12**, due to a supramolecular assembly of **5** and **12** with BXV<sup>4+</sup>,

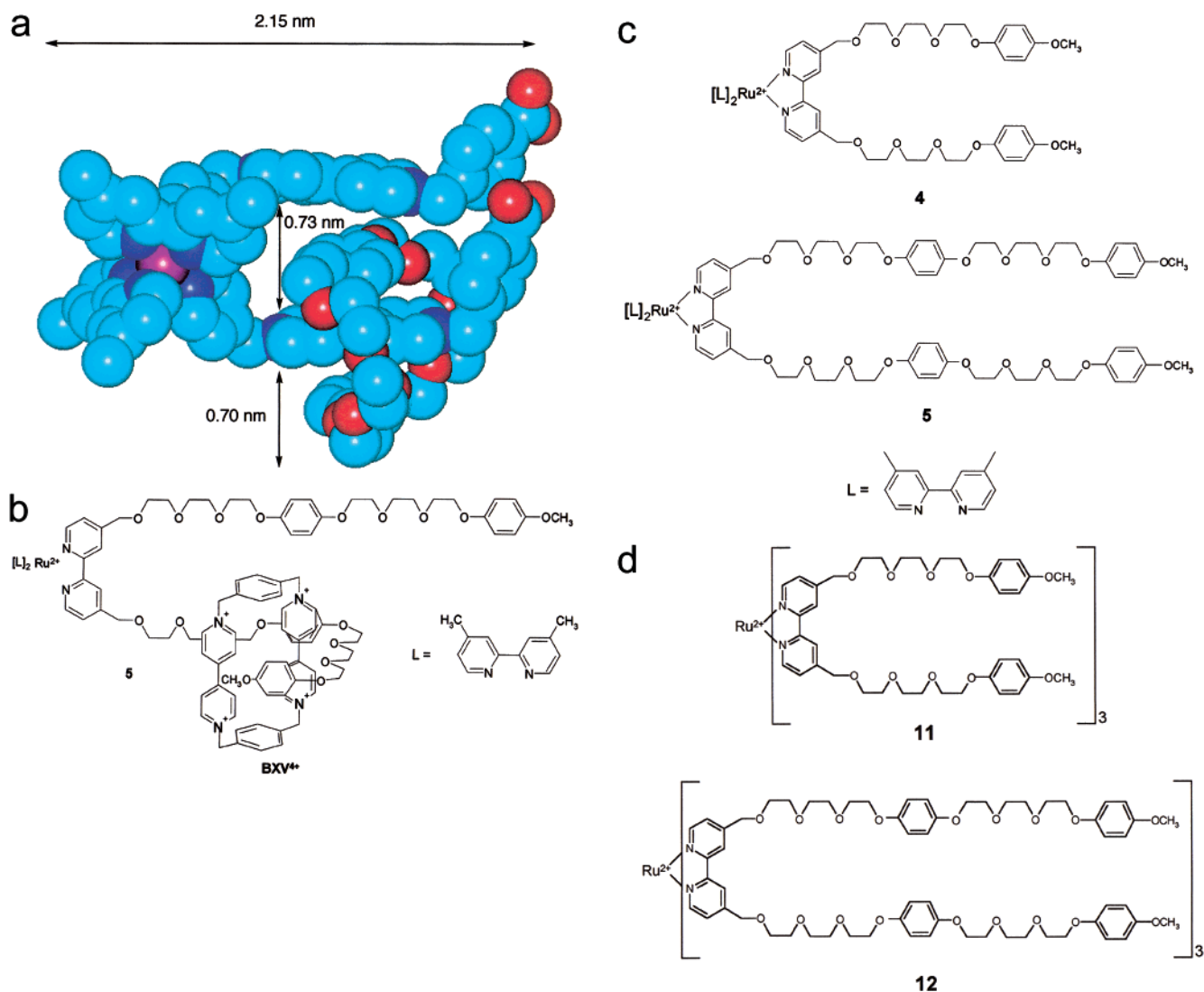
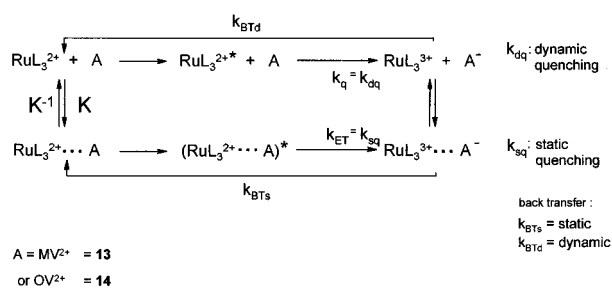


FIGURE 5. (a) MM<sup>+</sup>-minimized structure of two-shell complex showing a clear folding of the two-shell complex of **5** (Ru complex) + BXV<sup>4+</sup> (a) + (b). Structures of two- and four-shell **4** and **3** (c) and six-shell Ru complexes **11** and **12** (d).

Scheme 3



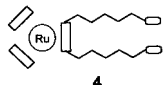
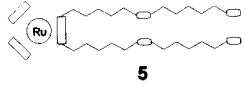
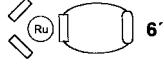
respectively. The time-resolved luminescence data of **4**, **5–11**, and **12** clearly showed a decrease of the initial luminescence as well as reduced lifetime  $\tau_1$  in the presence of BXV<sup>4+</sup> (eq 2). The quenching data demonstrated convincingly that the two-shell (two binding sites per branch) complexes **5** and **12** are quenched more efficiently by BXV<sup>4+</sup> than the one-shell complexes **4** and **11**. A faster time resolution resulted in a distinction of a fast and a slower diffusion-controlled quenching mode ( $k_{dq}$ ) (see Table 1 and kinetic Scheme 3). Using a statistical evalu-

ation, binding constants of the order of  $K = 110\text{--}210\text{ M}^{-1}$  (**5** and **12**) and  $10\text{--}20\text{ M}^{-1}$  (**4** and **11**) in CH<sub>3</sub>CN (**4** in water  $240\text{ M}^{-1}$ ) were determined (eq 3). A detailed probability calculation including the kinetic data showed the possibility for **5** and **12** to bind a maximum number of BXV<sup>4+</sup> (2 and 6), while for **4** and **11** the number of bound acceptors seems to be restricted to 1 or 2 relays BXV<sup>4+</sup>, respectively.<sup>24</sup> The time-resolved spectroscopy indicated a potential folding of the chains in **5** and **12**, which was responsible for the more efficient binding compared to that of **4** and **11**. This was substantiated also by NMR.<sup>22</sup>

## Mechanically or Catenane Linked Systems

We have prepared and studied a novel [2]catenane **A** incorporating cyclobis(paraquat-*p*-phenylene) (BXV<sup>4+</sup>) and 2,2'-bipyridine.<sup>26,27</sup> The complexation of this catenane within a ruthenium bis-complex affords an artificial photosynthesis assembly **6**, in which a sensitizer of

**Table 1. Dynamic Quenching Constants  $k_q$ , Intramolecular Quenching Constants  $k_{ET}$ , Association Constants  $K$ , Lifetime of Charge-Separated States  $\tau_{CS}$ , and Constants of Static Intramolecular Electron Back Transfer  $k_{BTs}$  of Ru(II) Complexes 4–6' in Acetonitrile in the Presence of 13 and 14**

Ru(II) complex	quencher	$k_q/L \text{ mol}^{-1} \text{ s}^{-1}$ ( $k_{ET}/s^{-1}$ )	$K/L \text{ mol}^{-1}$	$k_{BTs}/s^{-1}$ ( $\tau_{CS}/\text{ms}$ )	ref
 4	<b>13</b> (MV <sup>2+</sup> )	$0.17 \times 10^8$ <sup>a</sup>			23
	<b>14</b> (OV <sup>2+</sup> )	$1.21 \times 10^8$ <sup>a</sup>	$240 \pm 15$ <sup>a</sup>	$0.83 \times 10^6$ <sup>a</sup> (1200 <sup>a</sup> )	23
 5	<b>14</b>	$6.3 \times 10^8$ ( $2.2 \times 10^{11}$ ) <sup>b</sup>	$210 \pm 20$	$1\text{--}2 \times 10^6$ (600–800)	24
	<b>13</b>	$5.63 \times 10^8$ $1.83 \times 10^9$	$12 \pm 1$	(1) $4.98 \times 10^6$ (2) $\gg 1 \times 10^9$	29
 6'	<b>14</b>	$7.30 \times 10^8$	$119 \pm 14$	$4.76 \times 10^6$	29

<sup>a</sup> In water. <sup>b</sup>Intramolecular quenching K = from eq 3.

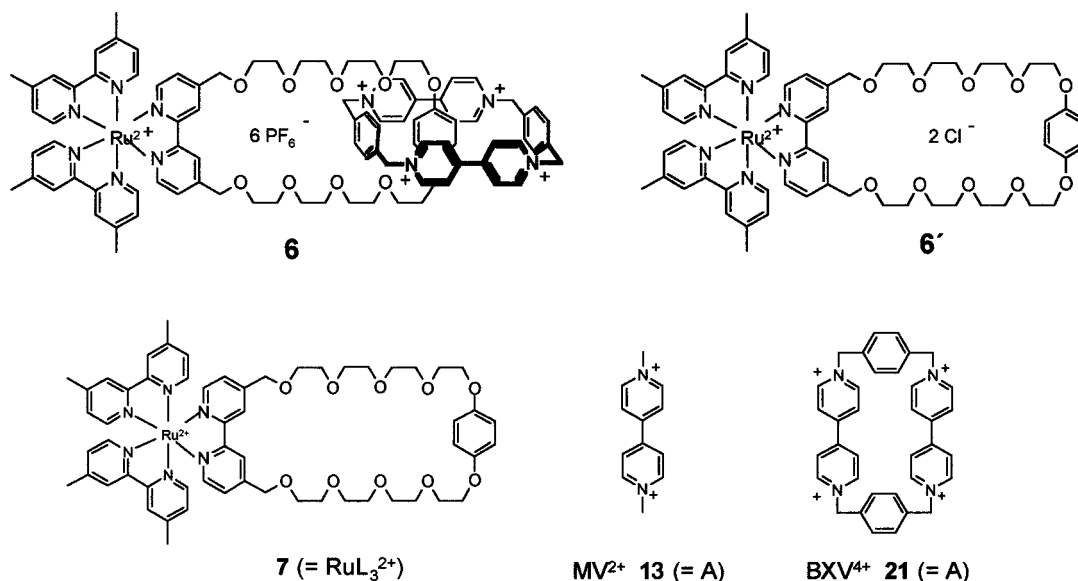


**FIGURE 6.** Structures of the [2]catenane complex **6** and the reference complex **6'**, **7**, **13**, and **21**.

type Ru(bpy)<sub>2</sub><sup>2+</sup> (bpy-polyether) **6'** and the cyclic bisviologen acceptor (BXV<sup>4+</sup>) are noncovalently linked (see Figure 6).

The catenane complex **6** has a structure related in principle to the photosynthetic reaction center. For the ligand **A** an X-ray analysis and a MM2 calculation were carried out. X-ray analysis and force field calculations differ slightly in geometry.<sup>26</sup>

Some important structural information on **6** was obtained from molecular modeling (see Figure 7). Interesting is the mean interplanar separation of the hydroquinone unit from the two 4,4'-bipyridinium systems, which are 4.64 and 5.19 Å, respectively. The extended conformation of the macrocyclic polyether in **6** causes a greater separation between the 2,2'-bipyridine system and the 4,4'-bipyridinium electron relay than in **A** (Figure 7).

Thus, the shortest distances between C-6-bpy and the cyclophane are 14.17 Å (**6a**) and 17.52 Å (**6b**) in the two conformations a and b.

## Electron-Transfer Studies

The emission data can be interpreted as the result of emission of a few conformers of **6** in which electron transfer is hindered by steric and donor–acceptor distance effects, although efficient intramolecular electron transfer occurs in most of the conformers of **6**. In our interpretation, the nanosecond emission observed for **6** comes mostly from the hindered processes, whereas the picosecond emission is assigned to efficient intramolecular electron transfer.

The rate of photoinduced electron transfer  $k_{ET}$  in the [2]catenane complex **6** is too high to be resolved by our instruments. However, it can be estimated roughly by inserting the emission data in eq 4:  $k_{ET} = (1/\tau_0)(\phi_0/\phi - 1)$ , in which  $\phi$  and  $\phi_0$  are the emission quantum yields of **6** and the reference **6'**, respectively, and  $\tau_0$  is the emission lifetime of **6'**.

The decay kinetics of **6**—determined by laser flash spectroscopy—are independent of the monitoring wavelength. We attribute the decay to the recombination of

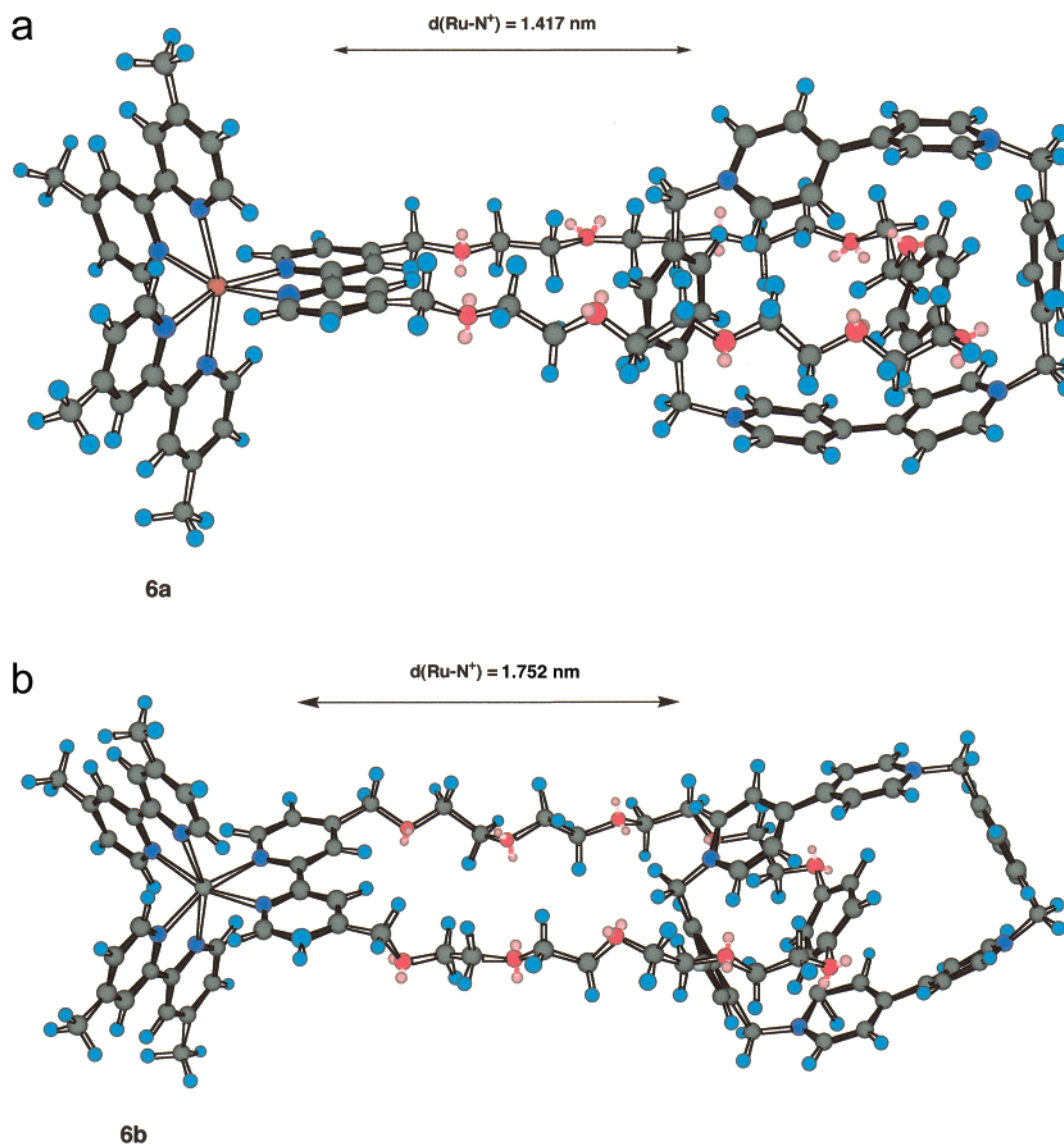


**FIGURE 7.** Molecular modeling results of the [2]catenane–ruthenium complex **6a** (close) and **6b** (extended) showing the two preferred conformations. The shortest distances between C-6-bpy and the cyclophane are 14.17 Å (**6a**) and 17.52 Å (**6b**) in the two conformations **a** and **b**.

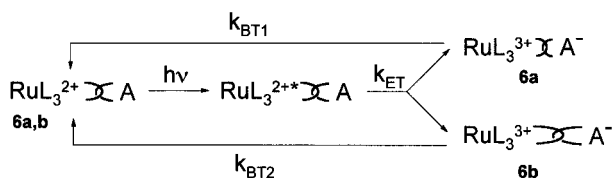


**FIGURE 8.** Kinetic scheme of electron-transfer processes in the [2]catenane complex **6**.

the redox products, that is, to back electron transfer from the reduced viologen to the oxidized chromophore  $\text{Ru}^{3+}$ –tris(bipyridine). As shown in Figure 8, the decay kinetics of the system are very different from the kinetics of the charge-separated state decays of covalently linked  $\text{Ru}^{2+}$ –tris(bipyridine)–bipyridinium systems and other covalently linked polyads. Two almost linear decays can be observed at both 610 and 380 nm (Figure 9), which in a biexponential fit afford lifetimes of the charge-separated state of  $\tau_{\text{CS1}} = 242 \pm 25$  ns (55 ± 3%) and  $\tau_{\text{CS2}} = 517 \pm 44$

ns (45 ± 3%), which lead to constants  $k_{\text{s}}$  for the back electron transfer of  $k_{\text{BT1}} = 4.13 \times 10^6$  s<sup>-1</sup> and  $k_{\text{BT2}} = 1.93 \times 10^6$  s<sup>-1</sup>, respectively. As indicated by molecular modeling and by electrochemical studies,<sup>26,27</sup> the different conformers of **6** can differ in their redox properties because of environmental effects. Accordingly, the two lifetimes can be ascribed to back electron transfer from reduced viologen to the oxidized metal center in these conformers of **6**, with alternative distances from the  $\text{BXV}^{4+}$  unit—and therefore from the viologen units—to the Ru center. In a straightforward approach, the shorter lifetime ( $\tau_{\text{CS1}} = 242 \pm 25$  ns) was assigned to back electron transfer from the reduced inside  $\text{BXV}^{4+}$  which is closer to the metal center, and the longer lifetime was assigned ( $\tau_{\text{CS2}} = 517 \pm 44$  ns) to that of the reduced outside  $\text{BXV}^{4+}$ .

The constants calculated<sup>26,27</sup> are  $k_{\text{ET}} > 2.1 \times 10^8$  s<sup>-1</sup> in water and  $k_{\text{ET}} > 2.6 \times 10^7$  s<sup>-1</sup> in  $\text{CH}_3\text{CN}$ , which are comparable with those obtained for pseudorotaxane-type

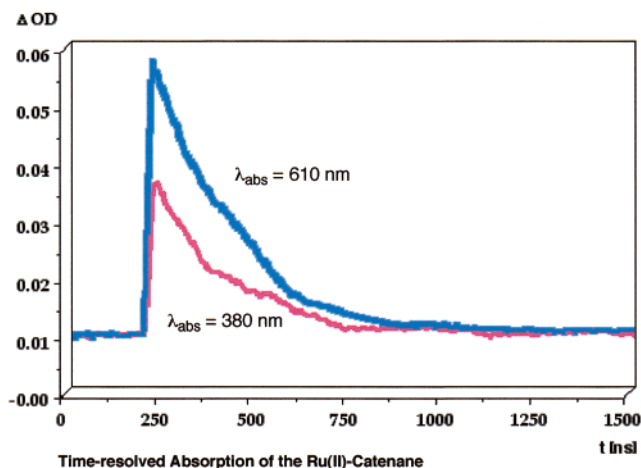


FIGURE 9. Decay of nanosecond transient of **6** (in acetonitrile,  $c = 2 \times 10^{-5} \text{ mol L}^{-1}$ ) recorded with laser flash spectroscopy.

Ru–tris(bipyridine)–BXV<sup>4+</sup> assemblies. These values should be the average for all the conformers of **6**. Studies with the reference complex **6'** and BXV<sup>4+</sup> revealed that a distinct luminescence lifetime quenching occurred only at higher concentrations of the acceptor (**6'**/BXV<sup>4+</sup> < 1:100). Here, dynamic quenching was predominant. Therefore, we conclude that the Ru<sup>2+</sup>–polypyridine catenane **6** can undergo efficient intramolecular electron transfer. Figure

9 shows the transient decays of the absorbance after pulsed laser excitation ( $\lambda = 532 \text{ nm}$ ) of **6** in water. There is absorbance at  $\lambda = 610$  and  $380 \text{ nm}$  characteristic of the radical cation of bipyridinium salts.

From femtosecond laser flash spectroscopy and single photon counting, two lifetimes were derived for **6**: (a) an extremely short  $\tau_L = 28 \text{ ps}$  and (b)  $\tau_L = 428 \text{ ns}$  in H<sub>2</sub>O (768 ns in acetonitrile). From femtosecond laser flash spectroscopy the rise times of the first transient were measured for **6**:  $\tau_1 = 180 \text{ fs}$  and  $\tau_2 = 14 \pm 1 \text{ ps}$ . It is remarkable that  $\tau_2$  is 6–7 times longer than the rise time for the singly and doubly branched covalent models **7** and **8** structures, vide infra in Figure 10.

The values found for **7** and **8** are in good agreement with Benniston's<sup>29a</sup> results of  $\tau_{CS} = 35 \pm 3 \text{ ps}$  for the catenane **15**, being very close to the value for complex **8**. A minor third transient ( $\phi = 5\%$ ) was found for **7**, **8**, and **9**.

## Covalently Linked Systems

Two-branched D–A assemblies come closer to the natural photosynthetic unit as mentioned earlier (vide supra). Therefore, model compounds of the types **8** and **9**<sup>21–25,28,30–32</sup> were designed to be good models for such studies. A monobranched D–A-diad **7**—in analogy to a

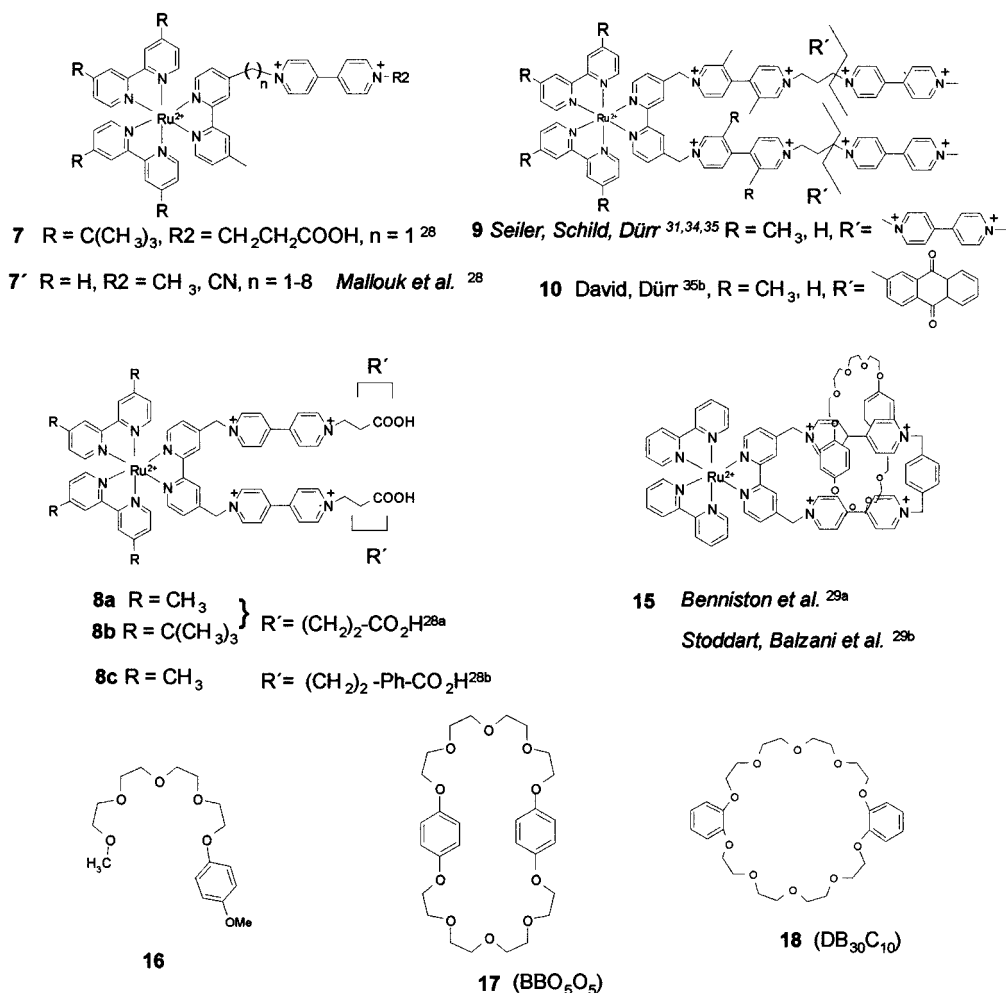


FIGURE 10. Structural formulas of covalently linked systems **7**–**10** and host **16**–**18**.



series of other studies—was included as a model compound. The spectral data were recorded and are characteristic for ruthenium polypyridines.<sup>28</sup> In this section mainly the results of time-resolved studies bearing on the electron-transfer processes will be dealt with. In general, in these polyads the D and A are linked by spacer groups. Compounds having D–A directly linked have been studied previously.<sup>33</sup>

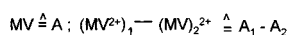
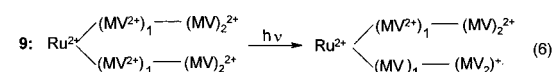
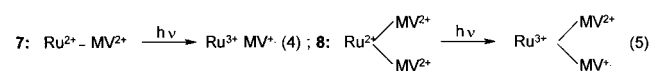
## Forward Electron Transfer

Transient spectra of the rise term recorded by femtosecond spectroscopy allowed a study of the forward electron transfer in **7**, **8**, and **9**.

For the diads **7** and **8**, an electron transfer within the exciting laser pulse is concluded, which may come from a <sup>3</sup>MLCT state or a hot <sup>1</sup>MLCT state. It is known that the <sup>3</sup>MLCT state in ruthenium polypyridines is populated in less than 1 ps.<sup>28</sup> The second term is then to be attributed to the electron transfer into the ligand. The electron probably will reside then in the electron-poor ligand, which is the viologen carrying a pyridine ring in this case. This process occurs in less than 6 ps, in good agreement with our data for **7** and **8**.<sup>28</sup> The rate constant for the whole process for **7** and **8** is roughly  $k_{ET} \approx 10^{11} \text{ s}^{-1}$ . **9** shows no picosecond transient, which indicates that this triad has a more complex electron-transfer mechanism, which leads to a longer lived charge-separated state of **9**.

## Charge Recombination

Product formation—in other words, the building up of the viologen radical cation—is represented in the following equations:



In steps (4)–(6) in the three compounds, the rise time of **7**, **8**, and **9** was monitored by femtosecond transient spectroscopy recorded at 610 nm (MV<sup>+</sup>, absorption maximum) (Table 2).

Employing a linear polyether **16** (Scheme 4) afforded the supramolecular assembly **9/16**.

The effect of the polyether giving a  $\tau_{CS} = 200 \mu\text{s}$  was originally explained by a rigidification of the assembly **9/16**.<sup>34</sup> The conformational mobility of the two arms in **9** should be reduced, and thus a more stretched out geometry of **9/16** would disfavor electron transfer.

A control experiment with TEOA (triethanolamine) as an additional donor in the system **9** afforded, however, also a very long-lived charge-separated state,  $\tau_{CS} = 212 \mu\text{s}$ .

Here an intermolecular mechanism comes into play. The high oxidation potential, TEOA = 0.85 V, quenches

**Table 2. Lifetime  $\tau_{CS}$  and Quantum Yields  $\phi_{CS}$  of Long-Lived Charge-Separated States of Ru(II) Diads **7**, **8a,b** and Triad **9** Compared to Models for the Photosynthetic Reaction Center**

complex <sup>a</sup> + electron donor	$\tau_{CS}/\mu\text{s}^b$	ref
<b>9</b> + <b>16</b>	220 <sup>b</sup>	30, 31, 36
<b>9</b> + TEOA	212 <sup>b</sup>	37
<b>7</b> + <b>16</b>	380 (~85%), 1072 (~15%) <sup>b</sup>	28
<b>7</b> + TEOA	293 (~95%), 1052 (~5%) <sup>b</sup>	28
<b>8</b> + <b>16</b>	163 <sup>b</sup>	28
<b>8</b> + <b>16</b>	197 <sup>b</sup>	28
<b>6</b> + TEOA	176 (~95%), 971 (~5%) <sup>b</sup>	28

<sup>a</sup> See the Charge Recombination section. <sup>b</sup> The quantum yield  $\phi_{CS}$  of viologen radical absorption was estimated to be  $\phi_{CS} = \sim 0.4$  (**9**),  $< 0.1$  (**7**, **8**, **6**), respectively (TEOA = triethanolamine).

the Ru<sup>\*/2+</sup> complex **9**. Thus, S\*–A<sub>1</sub><sup>2+</sup>–A<sub>2</sub><sup>2+</sup> is converted to S–A<sub>1</sub><sup>•+</sup>–A<sub>2</sub><sup>2+</sup>, which is further stabilized to S–A<sub>1</sub><sup>2+</sup>–A<sub>2</sub><sup>•+</sup>. A similar reduction is achieved with polyether **16**. This leads to a different mechanism in which the long-lived charge-separated state **9** exists in the ground state S<sup>+</sup>–A<sub>1</sub><sup>2+</sup>–A<sub>2</sub><sup>•+</sup>. A modified oxidative mechanism is operating. The anisylpolyether **16** cannot act as a donor ( $E_{1/2} = 1.37 \text{ V}$ ) for Ru<sup>3+/2+</sup>, and so electron transfer occurs in the sequence S\*–A<sub>1</sub><sup>2+</sup>–A<sub>2</sub><sup>2+</sup> → S<sup>+</sup>–A<sub>1</sub><sup>•+</sup>–A<sub>2</sub><sup>2+</sup> → S<sup>+</sup>–A<sub>1</sub><sup>2+</sup>–A<sub>2</sub><sup>•+</sup>. Now **16** can interfere as donor, giving a long-lived S<sup>+</sup>–A<sub>1</sub><sup>2+</sup>–A<sub>2</sub><sup>•+</sup>.

## Covalently Linked Systems Having Additional Noncovalent Interactions/Triads and Tetrads

The linear highly charged viologen units (A) in the new diads and triads allow an additional interaction with guests such as crown ethers. Using molecules with large cavities should allow the formation of a host–guest complex. We have investigated the host–guest chemistry of **7**, **8**, **9**, and **10** with crown ethers by NMR and molecular modeling (Figures 11 and 12).

The use of linear or cyclic polyethers on the ruthenium polyviologen complexes **7**, **8**, and **9** can have at least two effects:

(1) Conformational motions and special geometries can be restricted or changed (suppressed).

(2) The polyether may act as a potential donor.

Molecular modeling of **8** shows that a *p*-crown ether moiety **17** is residing halfway between the two viologen–pyridine rings. The aromatic rings of **17** are parallel to the viologen ring in a face-to-face arrangement, allowing for  $\pi$ – $\pi$  stacking.

In contrast to diads **8**, the triad forms a host–guest complex with crown ethers **17** and **18** in which the cyclic polyether resides on the terminal acceptor A<sub>2</sub>.

Molecular modeling of the assembly **9** and the cyclic ether **18** showed that, in principle, **9/18** = 1:1 and 1:2 complexes are geometrically possible. However, from NMR experiments we conclude rather a 1:1 complex **9/18**. The crown ether complexes with the terminal A<sub>2</sub> viologen, whereas according to NMR it complexes between A<sub>1</sub> and A<sub>2</sub> of **9**.

Similar results were obtained for the triad (dimetbpy)<sub>2</sub>–Ru<sup>2+</sup>V<sub>1</sub>–anthraquinone **10**.

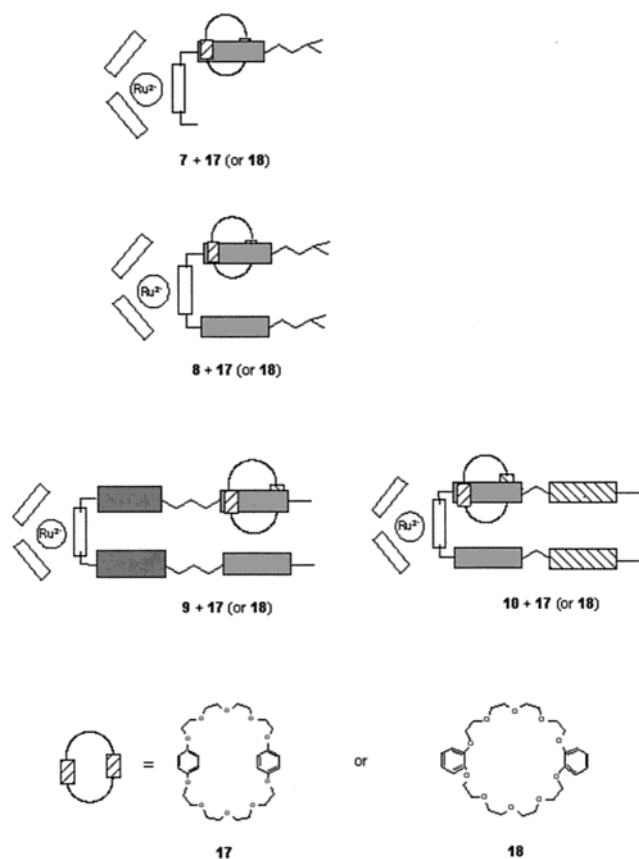


FIGURE 11. Schematic representation of the results of NMR titration of the pseudorotaxane assemblies of **7**–**10** and crown ethers.

## Electron-Transfer Studies of RuL<sub>3</sub> Complexes and Cyclic Ethers

Femtosecond laser spectroscopy showed that the rise term in the presence of the crown ethers **17** and **18** with **8b** and **9** is only little changed. However, the charge-separated state in the microsecond time domain shows large structure-dependent variations as indicated in Table 2.

From Table 2 one can clearly see that the binding constants with crown ether **17** are of the order of  $K_A = 146$ – $178 \text{ mol}^{-1}$  for **7**, **8a**, and **8b**. With **18**, having a smaller cavity, they are higher by a factor of 2. The lifetimes of the charge-separated states decrease in the following order: **17**,  $\tau_{cs}$  **8b** > **9** > **8a** > **7** and **18**,  $\tau_{cs}$  **7** > **9** > **8b** > **8a**.<sup>35</sup> The tetrad assemblies **9** and **17** or **18** show, however, the highest quantum efficiencies.<sup>36–40</sup>

## Photoinduced Electron Transfer in the Marcus Inverted Region

The Marcus formalism<sup>41</sup> reveals a remarkable insight into the basic electron-transfer mechanisms of the diads **7** and **8**, the triad **9**, and the [2]catenane–ruthenium(II) complex **6**.

The classic Marcus formalism relates the observed electron-transfer rate constants,  $k_{et}$ , with the free energies,  $\Delta G^\circ$ , of the forward and back electron-transfer reactions. The reorganization energy  $\lambda$  is necessary for the structural

reorganization of the (photo)donor, the acceptor, and their solvation spheres upon electron transfer.  $k_{et}(0)$  is the maximal (activationless) electron-transfer rate constant, which can be observed when  $-\Delta G^\circ = \lambda$  ( $k_b$ , the Boltzmann constant). Note that Marcus behavior (Figure 13) was increased when supramolecular complexation of the investigated diads and triads with the cyclic crown ethers **17** BBO<sub>5</sub>O<sub>5</sub> and **18** DB<sub>30</sub>C<sub>10</sub> took place.<sup>28,35</sup> In this case, especially long lifetimes of charge separation upon laser irradiation ( $\lambda_{ex} = 532 \text{ nm}$ ) were detected (up to  $212 \mu\text{s}$  in the case of triad **9**) complexed with DB<sub>30</sub>C<sub>10</sub>. A reorganization energy of  $\lambda = 1.1 \pm 0.05$  fits the two sets of electron-transfer data, (a) and (b). When crown ether complexation occurred, (a) remained unchanged within experimental error, whereas a new data set (c) was measured for the back-transfer of the crown ether complex diads and triad, reducing  $\lambda$  to  $0.96 \pm 0.05$ . Consequently, crown ether complexation of the diads and triads leads to a reduction of reorganization energy  $\lambda$ , resulting in a reduction of the rate of charge recombination. This means that only one of the two viologen branches of the diads and the triad is complexed by the crown ether moiety and that the electron is located on the complexed viologen branch.<sup>28</sup> The forward electron transfer proceeds with approximately the same probability to both viologen branches, as shown by the quantum efficiencies for charge separation  $\Phi_{cs} = 0.4 \pm 0.03$  (triad **9**) to  $\Phi_{cs} = 0.05 \pm 0.008$  (diads **7**, **8**).<sup>28</sup> However, only the electron-transfer process to the crown ether-complexed viologen units leads to long-lived charge-separated states.

In Table 3 the lifetimes of charge-separated states  $\tau_{cs}$  and quantum yields  $\phi_{cs}$  of the best literature systems and our work are compared. It becomes evident that the supramolecular assembly **9**/polyether is among the best systems known today.

## Conclusions

Simple Ru complexes having polyether bipyridines as building blocks, such as in ruthenium popydates and ruthenium coronates, were shown to be among the most photostable Ru complexes prepared so far.

- The fine-tuning of molecular properties in these ruthenium polypyridines allows for the design of structures which are well suited for electron transfer.

Two-shell biomimetic model systems, such as the noncovalent supramolecular assembly (**5**/BXV<sup>4+</sup>), display more efficient electron transfer than one-shell systems.

- Covalently linked assemblies<sup>7–9</sup> are, however, more efficient in electron transfer.

- Assemblies using covalent interactions of ruthenium polypyridines forming pseudorotaxanes such as triads and tetrads are among the most efficient systems to produce a charge-separated D<sup>+</sup>–A<sup>–</sup> state.

- A comparison of the three concepts of (a) noncovalently, (b) mechanically, and (c) covalently linked D–A diads, triads, and tetrads shows that, with regard to formation of the charge-separated states, noncovalently

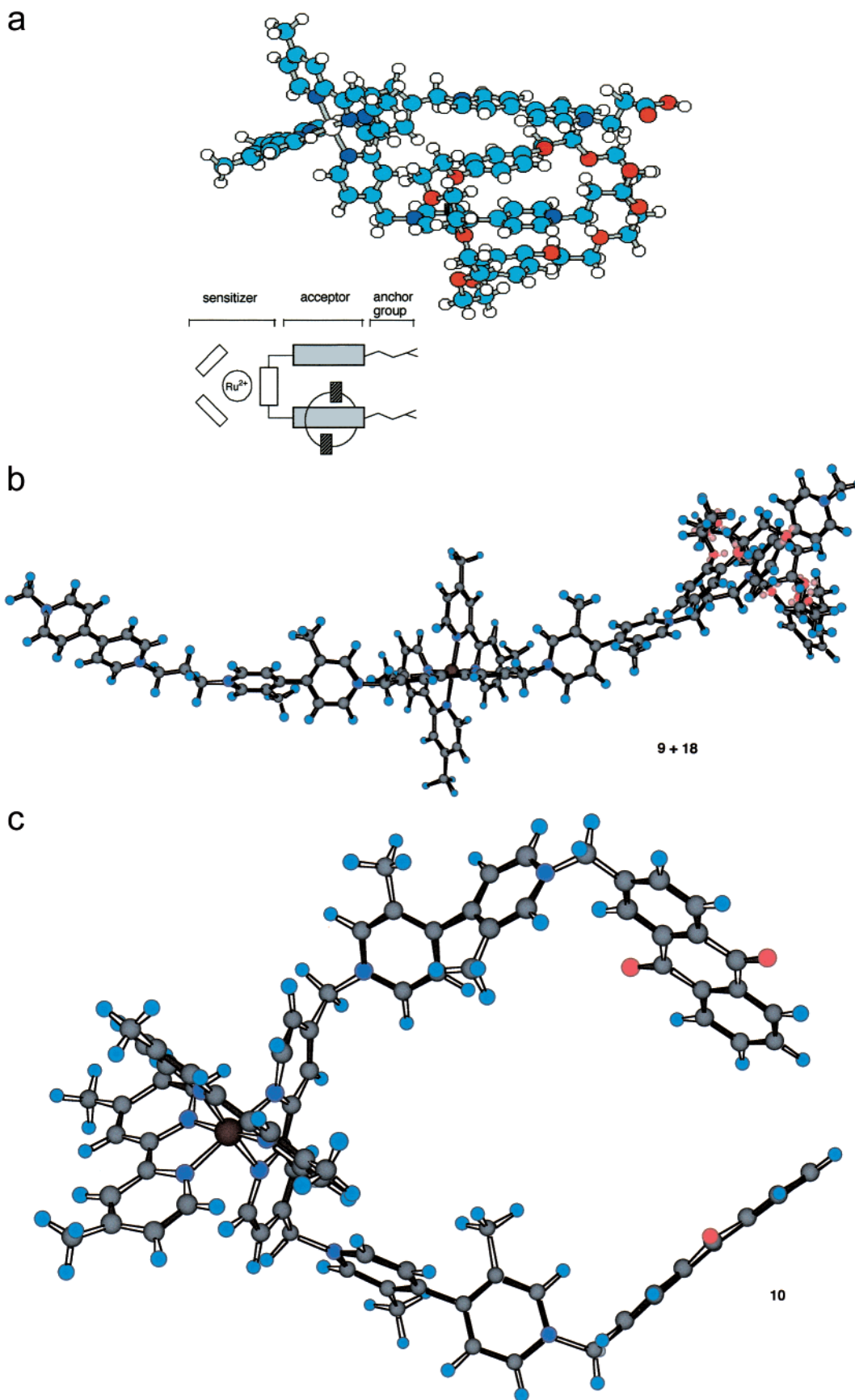


**FIGURE 12.** (a) Molecular modeling of diad **8**/crown ether **17**: assembly for the typical 1:1 complex. (b) MM/2 calculation (enhanced parameter set) of triad **9**/crown ether **18** assembly (1:1 complex) demonstrating a linear-shaped very extended geometry. (c) MM/2 calculation (enhanced parameter set) of triad **10** showing a preferred conformation pointing out the interaction of the anthraquinone subunits.<sup>35b</sup>

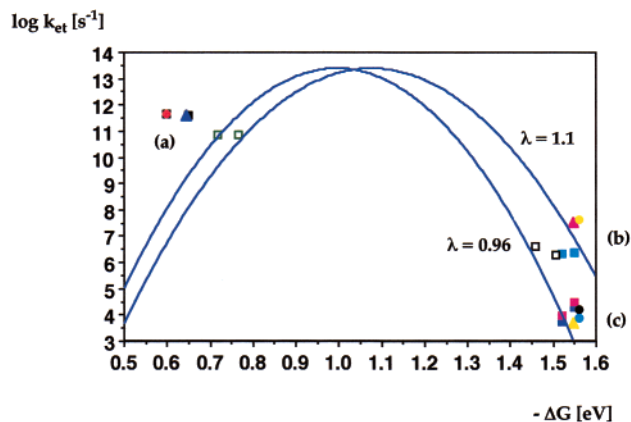


**FIGURE 13.** Marcus plot of the observed electron-transfer rates versus the free energy driving force for the electron transfer occurring within the diads, the triad, and the [2]catenane–ruthenium(II) complex in H<sub>2</sub>O (filled squares, diads **7**, **8**; filled circle, monodiad **7**; filled triangle, triad **9**; open square, [2]catenane–ruthenium(II) complex **6**). The calculated fits from eq 5 (using  $k_{\text{et}}(0) = 3.15 \times 10^{13} \text{ s}^{-1}$  and  $\lambda = 1.1$  as well as and  $\lambda = 0.96$ ) indicate the different kinetics of the free and crown ether-complexed diads and triad. (a) Photoinduced electron-transfer rates; (b) back-transfer rates of the [2]catenane–ruthenium(II) complex **6** and the free diads **7**, **8** and triad **9**, and (c) back-transfer rates of the diads and triad, complexed with the cyclic crown ethers **17** BBO<sub>5</sub>O<sub>5</sub> and **18** DB<sub>30</sub>C<sub>10</sub>.

**Table 3. Comparison of Charge Separation in Artificial Systems**

system	$\tau_{\text{CS}}$ ( $\phi_{\text{CS}}$ )
reaction center	100 ms ( $\sim 1$ ) <sup>b</sup>
bacterial photosynthetic <sup>37</sup>	10 ns ( $\sim 1$ ) <sup>a</sup>
pentad <sup>c</sup> (Gust, Moore et al.) <sup>37</sup>	340 $\mu\text{s}$ (0.15)
tetrad <sup>d</sup> (Paddon-Row et al.) <sup>38</sup>	32 $\mu\text{s}$ (0.23)
C <sub>60</sub> triad <sup>e</sup> (Gust, Moore et al.) <sup>39</sup>	170 ns (0.14)
triad <sup>f</sup> (Sauvage et al.) <sup>40</sup>	33 ns ( $-$ )
triad <b>9</b> + <b>16</b> (Seiler, Dürre et al.) <sup>30,31,34,35</sup>	220 $\mu\text{s}$ ( $\sim 0.4$ )
diad <b>8a</b> + <b>17</b> <sup>28</sup>	104 $\mu\text{s}$ ( $\sim 0.05$ )
diad <b>8b</b> + <b>17</b> <sup>28</sup>	187 $\mu\text{s}$ ( $\sim 0.05$ )
diad <b>7</b> + <b>18</b> <sup>28</sup>	136 $\mu\text{s}$ ( $\sim 0.1$ )
[2]Catenane <b>6</b> <sup>26,27</sup>	242 ns (55%)
	517 ns (45%)

<sup>a</sup> Recombination of special pair<sup>+</sup>/bacteriopheophytin<sup>-</sup>. <sup>b</sup> Recombination of special pair<sup>+</sup>/quinone a<sup>-</sup>. <sup>c</sup> Zn-porphyrin, porphyrin, naphtho- and benzoquinone, carotene. <sup>d</sup> Dimethoxyamino-naphthalene, dimethylaminobenzene, dicyanovinylidene. <sup>e</sup> Fullerene, carotene. <sup>f</sup> Zn- and Au-porphyrin, Ru-terpyridine.

< mechanically < covalently linked D–A assemblies are increasingly efficient.

It can thus be generalized that the study of biomimetic systems based on ruthenium polypyridines leads to highly efficient electron-transfer systems. Some of the recently studied covalent/noncovalent RuL<sub>3</sub> pseudorotaxanes (**7** or **9** and cyclic ether **17**, **18**) are among the best systems for electron transfer known today. They compare nicely to the porphyrin tetrads and pentads of Gust et al.<sup>7b,37,39</sup> and the push–pull systems of Paddon–Row,<sup>38</sup> which are very sophisticated systems, however made in complex syntheses. Future studies in the field of biomimetic artificial photosynthesis systems should be, as this Account shows, not in the domain of the often beautiful noncovalent assemblies but clearly on the covalently linked systems, which are clearly the superior systems.

This work has been supported by the BMFT and the Volkswagen Stiftung, and financial help is greatly appreciated. Our special thanks are due to the groups of A. M. Braun (Universität Karlsruhe), F. De Schryver (Universität Leuven), N. J. Turro (Columbia University, New York) and I. Willner (Hebrew University, Jerusalem) for laser nanosecond, picosecond, and femtosecond spectroscopy. H.D. expresses his sincere thanks to all the co-workers involved in this project. All of them have been cited in this report.

## References

- (1) Barber, J.; Andersson, B. *Nature* **1994**, *370*, 31–34.
- (2) Yachandra, V. K.; Sauer, K.; Klein, M. P. *Chem. Rev.* **1996**, *96*, 2927–2950.
- (3) Deisenhofer, J.; Epp, O.; Sinning, I.; Michel, H. Crystallographic Refinement at 2.3 Å Resolution and Refined Model of the Photosynthetic Reaction Centre from *Rhodospseudomonas viridis*. *J. Mol. Biol.* **1995**, *246*, 429–458.
- (4) Balzani, V.; De Cola, L., Eds. *Supramolecular Chemistry*; NATO ASI Series; Kluwer Academic Publishers: Dordrecht, 1992.
- (5) (a) Juris, A.; Barigelletti, F.; Campagna, S.; Balzani, V.; Belser, P.; Zelewsky, A. Ruthenium(II)polypyridine complexes: photophysics, photochemistry, electrochemistry and chemiluminescence. *Coord. Chem. Rev.* **1988**, *84*, 85–277. (b) Balzani V.; Scandola F. *Supramolecular Photochemistry*; Horwood: Chichester, 1990. (c) Kiwi, J.; Kalyanasundaram, K.; Graetzel, M. Visible light induced cleavage of water into hydrogen and oxygen in colloidal and microheterogeneous systems. *Struct. Bonding* **1981**, *49*, 37–125.
- (6) (a) Reviews: Dürre, H. *Artifizielle Photosynthese*. *Mag. Forschung Uni des Saarlandes* **1989**, *1*, 62–72. (b) Dürre H.; Bossmann S.; Kilburg H.; Trierweiler H. P.; Schwarz R. In *Frontiers in Supramolecular Organic Chemistry and Photochemistry*; Dürre, H., Schneider, H. J., Eds.; VCH: Weinheim, 1991. (c) Dürre, H.; Bossmann, S. H.; Schwarz, R.; Kropf, M.; Hayo, R.; Turro, N. J. *Supramolecular Assemblies for Light Induced Electron-Transfer Reactions*. *J. Photochem. Photobiol. A: Chem.* **1994**, *80*, 341–350. (d) Dürre, H.; Bossmann S. H.; Heppe, G.; Schwarz, R.; Thiery, U.; Trierweiler, H. P. Light induced electron transfer in simple and supramolecular Ru-polypyridine complexes. *Proc. Indian Acad. Sci., Chem. Sci.* **1993**, *105*, 435–450.
- (7) (a) Dürre, H.; Dörr, G.; Zengerle, K.; Mayer, E.; Curchod, J. M.; Braun, A. M. Possibilités et limites des diazacomplexes de Ru<sup>2+</sup> entant que sensibilisateurs induisant la photolyse de l'eau. *Nouv. J. Chim.* **1985**, *9*, 717–720. (b) Gust, D.; Moore, T. A.; Moore, A. L. Mimicking bacterial photosynthesis. *Pure Appl. Chem.* **1998**, *70*, 2189–2200. (c) Sessler, J. L.; Wang, B.; Harriman, A. Photo-induced energy transfer in associated, but noncovalently linked photosynthetic model systems. *J. Am. Chem. Soc.* **1995**, *117*, 704–714. (d) Wasielewski, M. R. Photoinduced Electron Transfer in Supramolecular Systems for Artificial Photosynthesis. *Chem. Rev.* **1992**, *92*, 435–462.
- (8) Tiecco, M.; Testaferri, L.; Tingoli, M.; Chianelli, D.; Montanucci, M. A. Convenient synthesis of bipyridines by nickel-phosphine complex-mediated homo coupling of halopyridines. *Synthesis* **1984**, *9*, 736–738.
- (9) Dürre, H.; Willner, I.; Maidan, R. Photosensitized reduction of CO<sub>2</sub> to CH<sub>4</sub> and H<sub>2</sub> evolution in the presence of Ruthenium and Osmium colloids. *J. Am. Chem. Soc.* **1987**, *109*, 6080–6086.
- (10) Dürre, H.; Zengerle, K.; Trierweiler, H. P. Podanden, Coronanden und Kryptanden als neue Komplex-Liganden für Photoelektronentransfer-Reaktionen. *Z. Naturforsch. B* **1988**, *43*, 361–367.
- (11) Dürre, H.; Kilburg, H.; Bossmann S. H. Efficient synthesis of crown ester-linked Ru-complexes: a new class of supramolecular sensitizer-crown ester assembly for electron transfer. *J. Synth. Org. Chem.* **1990**, *9*, 773–781.
- (12) Dürre, H.; Trierweiler, H. P.; Willner, I.; Maidan, R. Application of Ru(II)-polypyridine sensitizers in the reduction of CO<sub>2</sub> to CH<sub>4</sub> and H<sub>2</sub>-evolution using Ru-colloids. *New J. Chem.* **1990**, *14*, 317–320.
- (13) Dürre H.; Schwarz R. Photosensibilisatoren hoher Stabilität und Verfahren zu ihrer Herstellung. *Deutsche Offenlegungsschrift T 42 17588*, 1992, 7–44.
- (14) Dürre, H.; Bossmann, S. H. Crownether—A new type of photostable linked Ru-coronates electron-transfer sensitizer. *New J. Chem.* **1992**, *16*, 769–770.
- (15) Dürre, H.; Willner, I.; Schwarz, R. Formation of supramolecular complexes of Ru(II)tris-oligoethyleneglycol-bipyridine with alkali and alkaline earth metal ions. *J. Chem. Soc., Chem. Commun.* **1992**, *18*, 1338–1339.

- (16) Dürre, H.; Bossmann, S. H.; Beuerlein, A. Biomimetic approaches to the construction of supramolecular catalysts: titanium-dioxide-platinum antenna catalysts to reduce water using visible light. *J. Photochem. Photobiol. A: Chem.* **1993**, *73*, 233–245.
- (17) Dürre, H.; Bossmann, S. H.; Mayer, E. Biomimetische Photosysteme zur sakrifiziellen Wasserreduktion. *Z. Naturforsch.* **1993**, *48b*, 369–386.
- (18) Dürre, H.; Schwarz, R.; Andreis, C.; Willner, I. Highly photostable sensitizers for artificial photosynthesis. Ru(II)-3,3-bis(diazine)-6,6'-oligo(ethylene-glycol)-complexes and a new class of podates. *J. Am. Chem. Soc.* **1993**, *115*, 12362–12365.
- (19) Dürre, H.; Bossmann, S. H.; Seiler, M. Supramolecular sensitizers relay assemblies: an evolution of binding constants from new linear Stern–Volmer plots. *J. Phys. Org. Chem.* **1992**, *13*, 63–70.
- (20) Dürre, H.; Bossmann, S. H.; Schwarz, R. Supramolekulare Sensibilisatoren zum photo-induzierten Elektronentransfer. *J. Inf. Rec. Mater.* **1994**, *21*, 471–474.
- (21) Kropf, M.; Dürre, H.; Collet, C. Preparation of new octopus shaped homoleptic and heteroleptic Ru(II)-bisdiazine complexes. *Synthesis* **1996**, *5*, 609–614.
- (22) Dürre, H.; David, E.; Seiler, M. Model Systems for Artificial Photosynthesis, Supramolecular Relays Assemblies. *J. Inf. Rec.* **1996**, *22*, 417–419.
- (23) Kropf, M.; Joselevich, E.; Dürre, H.; Willner, I. Photoinduced Electron-Transfer in Supramolecular Assemblies Composed of Alkoxy-anisyl tethered Ru(II)-trispyridazine Complexes and a Bipyridinium-Cyclophane Electron Acceptor. *J. Am. Chem. Soc.* **1996**, *118*, 655–665.
- (24) David, E.; Born, R.; Kaganer, E.; Joselevich, E.; Dürre, H.; Willner, I. Photoinduced Electron Transfer in Supramolecular Assemblies Composed of One-Shell and Two-Shell Dialkoxybenzene-Tethered Ru(II)-Tris(bipyridine) Derivatives and a Bipyridinium Cyclophane. *J. Am. Chem. Soc.* **1997**, *33*, 7778–7790.
- (25) Zahavy, E.; Seiler, M.; Marx-Tibbon, S.; Joselevich, E.; Willner, I.; Dürre, H.; O'Connor, D.; Harriman, A. Effective Charge Separation in Intermolecular Complexes of an Electron Donor and a Doubly Branched Triad Assembly: A Model System for Environmental Effects Controlling Electron Transfer. *Angew. Chem.* **1995**, *107*, 1112–1114; *Angew. Chem., Int. Ed. Engl.* **1995**, *34*, 1005–1007.
- (26) Hu, Y.; van Loyen, D.; Schwarz, O.; Bossmann, S. H.; Dürre, H.; Huch, V.; Veith, M. Intramolecular Electron Transfer between Noncovalently Linked Donor and Acceptor in a [2]Catenane. *J. Am. Chem. Soc.* **1998**, *120*, 5822–5823.
- (27) Hu, Y.; Bossmann, S. H.; van Loyen, D.; Schwarz, O.; Dürre, H. A Novel 2,2'-Bipyridine[2]catenane and its Ruthenium Complex: Synthesis, Structure and Intramolecular Electron Transfer—A Model for the Photosynthetic Reaction Center. *Chem. Eur. J.* **1999**, *5*, 1267–1277.
- (28) van Loyen, D., Thesis, Universität des Saarlandes, 1999.
- (29) (a) Benniston, A. C.; Mackie, P. R.; Harriman, A. Künstliche Photosynthese: Nachahmung der Redoxasymmetrie. *Angew. Chem.* **1998**, *110*, 354–355; *Angew. Chem., Int. Ed. Engl.* **1998**, *37*, 376–378. (b) Ashton, P. R.; Ballardini, R.; Balzani, V.; Constable, E. C.; Credi, A.; Kocian, O.; Langford, S. J.; Prodi, L.; Schofield, E. R. Ru(II)-Polypyridine Complexes Covalently Linked to Electron Acceptors as Wires for Light-Driven Pseudorotaxane-Type Molecular Machines. *Chem. Eur. J.* **1998**, *4*, 2413–2422. (c) Yonemoto, E. H.; Kim, Y. I.; Schmeihl, R. H.; Wallin, J. O.; Shoulders, B. A.; Richardson, B. R.; Haw, J. F.; Mallouk, T. E. Photoinduced Electron-Transfer Reactions in Zeolite-Based Donor–Acceptor and Donor–Donor–Acceptor Diads and Triads. *J. Am. Chem. Soc.* **1994**, *116*, 10557–10563.
- (30) Kropf, M.; van Loyen, D.; Schwarz, O.; Dürre, H. Biomimetic Models of the Photosynthetic Reaction Center Based on Ruthenium-Polypyridine Complexes. *J. Phys. Chem. A* **1998**, *102*, 5499–5505.
- (31) Seiler, M.; Dürre, H. Modellsysteme zur artifizialen Photosynthese—Synthese und Elektronentransferstudien neuartiger Sensibilisator-Relais-Einheiten. *Liebigs Ann.* **1995**, 407–413.
- (32) Seiler, M.; Dürre, H. Synthesis of a New Type Sensitizer-Relay-Triad: Model Compounds for Artificial Photosynthesis. *Synthesis* **1994**, *1*, 83–86.
- (33) Dürre, H.; Thiery, U.; Infelta, P.; Braun, A. M. Sensitizer-Relay Assembly for Electron-Transfer Processes. *New J. Chem.* **1989**, 8–9.
- (34) Seiler, M. Thesis, Universität des Saarlandes, 1994.
- (35) (a) Schild, V., Thesis, Universität des Saarlandes, 2000. (b) David, E. D., Thesis, Universität des Saarlandes, 1998.
- (36) Abresch, E. C.; Paddock, M. L.; Stowell, M. H. B.; McPhillips, T. M.; Axelrod, H. L.; Soltis, S. M.; Rees, D. C.; Okamura, M. Y.; Feher, G. Identification of proton-transfer pathways in the X-ray crystal structure of the bacterial reaction center from *Rhodospirillum rubrum*. *Photosynth. Res.* **1998**, *55*, 119–125.
- (37) Gust, D.; Moore, T. A.; Moore, A. L. Molecular mimicry of photosynthetic energy and electron transfer. *Acc. Chem. Res.* **1993**, *26*, 198–205.
- (38) Jolliffe, K. A.; Bell, T. D. M.; Ghiggino, K. P.; Langford, S. J.; Paddon-Row, M. N. Efficient Photoinduced Electron Transfer in a Rigid U-Shaped Tetrad Bearing Terminal Porphyrin and Viologen Units. *Angew. Chem.* **1998**, *110*, 960–963; *Angew. Chem., Int. Ed. Engl.* **1998**, *37*, 916–919.
- (39) Liddell, P. A.; Kuciauskas, D.; Sumida, J. P.; Nash, B.; Nguyen, D.; Moore, A. L.; Moore, T. A.; Gust, D. Photoinduced Charge Separation and Charge Recombination to a Triplet State in a Carotene-Porphyrin-Fullerene Triad. *J. Am. Chem. Soc.* **1997**, *119*, 1400–1405 and earlier work.
- (40) Harriman, A.; Odobel, F.; Sauvage, J. P. Multistep Electron Transfer in a Porphyrin-Ruthenium(II)Bis(terpyridyl)-Porphyrin Triad. *J. Am. Chem. Soc.* **1994**, *116*, 5481–5482.
- (41) Turro, C.; Zalesky, J. M.; Karabatsos, Y. M.; Nocera, D. G. Biomolecular Electron Transfer in the Marcus Inverted Region. *J. Am. Chem. Soc.* **1996**, *118*, 6060–6067.

AR9901220